Glodny, J., Echtler, H., Collao, S., Ardiles, M., Burón, P., Figueroa, O. (2008): Differential Late Paleozoic active margin evolution in South-Central Chile (37°S-40°S) -The Lanalhue Fault Zone. - Journal of South American Earth Sciences, 26, 4, 397-411

DOI: 10.1016/j.jsames.2008.06.001.

Accepted Manuscript

Differential Late Paleozoic active margin evolution in South-Central Chile (37°S-40°S) -The Lanalhue Fault Zone

Johannes Glodny, Helmut Echtler, Santiago Collao, Mary Ardiles, Pablo Burón, Oscar Figueroa

PII: S0895-9811(08)00053-9
DOI: 10.1016/j.jsames.2008.06.001
Reference: SAMES 759

To appear in: *Journal of South American Earth Sciences*

Received Date: 17 January 2008
Accepted Date: 5 June 2008

Please cite this article as: Glodny, J., Echtler, H., Collao, S., Ardiles, M., Burón, P., Figueroa, O., Differential Late Paleozoic active margin evolution in South-Central Chile (37°S-40°S) -The Lanalhue Fault Zone, *Journal of South American Earth Sciences* (2008), doi: 10.1016/j.jsames.2008.06.001

Differential Late Paleozoic active margin evolution in South-Central Chile (37°S-40°S) - The Lanalhue Fault Zone

Johannes Glodny[1]*, Helmut Echtler[1], Santiago Collao[2],
Mary Ardiles[2], Pablo Burón[2], Oscar Figueroa[2]

(1) GeoForschungsZentrum Potsdam, Telegrafenberg C2, D-14473 Potsdam, Germany
(2) Departamento Ciencias de la Tierra, Universidad de Concepción, Casilla 2-D, Concepción, Chile

*: Corresponding author: Johannes Glodny
Phone: +49 331 2881375
Fax: +49 331 2881370;
e-mail: glodnyj@gfz-potsdam.de

Abstract

The N-S oriented Coastal Cordillera of South Central Chile shows marked lithological contrasts along strike at ~38°S. Here, the sinistral NW-SE-striking Lanalhue Fault Zone (*nomen novum*) juxtaposes Permo-Carboniferous magmatic arc granitoids and associated, frontally accreted metasediments (Eastern Series) in the northeast with a Late Carboniferous to Triassic basal-accretionary forearc wedge complex (Western Series) in the southwest. The fault is interpreted as an initially ductile deformation zone with divergent character, located in the eastern flank of the basally growing, upwarping, and exhuming Western Series. It was later transformed and reactivated as a semiductile to brittle sinistral transform fault. Rb-Sr data and fluid inclusion studies of late-stage fault-related mineralizations revealed Early Permian ages between 280 and 270 Ma for fault activity, with subsequent minor erosion. Regionally, crystallization of arc intrusives and related metamorphism occurred between ~306 and ~286 Ma, preceded by early increments of convergence-related deformation. Basal Western Series accretion started at >290 Ma and lasted to ~250 Ma. North of the Lanalhue fault, Late Paleozoic magmatic arc granitoids are nearly 100 km closer to the present day Andean trench than further south. We hypothesize that this marked difference in paleo-forearc width is due to an Early Permian period of subduction erosion north of 38°S, contrasting with ongoing accretion further south, which kinematically triggered the evolution of the Lanalhue Fault Zone. Permo-Triassic margin segmentation was due to differential forearc accretion and denudation characteristics, and is now expressed in contrasting lithologies and metamorphic signatures in todays Andean forearc region north and south of the Lanalhue Fault Zone.

Keywords: forearc deformation, accretion, tectonic erosion, isotopic dating, Permian, Chile

1. Introduction

The Coastal Cordillera of South Central Chile is dominated by Upper Carboniferous to Triassic crystalline basement. Petrologic work has documented marked contrasts in the composition and metamorphic evolution of this basement across a NW-SE striking, lineament-like fault zone within the Cordillera Nahuelbuta (Fig. 1). Northeast of this fault zone, i.e., north of ~38°S, Upper Carboniferous to Early Permian granitoids are associated with metasediments, termed 'Eastern Series', which show distinct, very low-grade, medium pressure to HT-LP contact-metamorphic overprints (Aguirre et al., 1972; Hervé, 1977; Kato, 1985; Willner et al., 2000; Lucassen et al., 2004). Southwest of the lineament, the Coastal Cordillera is made up of a Permotriassic forearc accretionary wedge known as 'Western Series'. Its intercalated metasediments and metabasites show a distinct high P / low T signature, with a regionally homogeneous metamorphic grade of transitional greenschist- to blueschist facies (Aguirre et al., 1972; Hervé, 1988; Willner et al., 2001; Willner, 2005; Glodny et al., 2005).

On a larger scale, the contact between Western and Eastern Series has been recognized as a major crustal discontinuity due to the associated lithological contrasts (Ernst, 1975; Kato, 1976, 1985; Hervé, 1977). Western and Eastern Series have been interpreted as near-contemporaneous and genetically associated, constituting a paired metamorphic belt (sensu Miyashiro, 1961; Aguirre et al., 1972; Ernst, 1975). The contact between the Western and Eastern Series can be traced or inferred for more than 1000 km south of ~34°S. The nature of this contact is regionally variable, from transitional (on a km scale) to tectonic (Davidson et al., 1987; Richter et al., 2007) The NW-SE striking segment at ~38°S is unique in that it is the only segment where this contact significantly deviates from a trench-parallel, NNE-SSW orientation (Fig. 1). The first-order fault zone at ~38°S is thus a key tectonic feature for a better understanding of the regional forearc basement architecture.

The exact age and tectonic nature of fault activity has so far been unknown (cf. Martin et al., 1997, 1999), leaving open questions about the geodynamic role of this fault zone. Beside reference to it as the regional 'Eastern Series-Western Series contact', a variety of names exist in the literature. While the term 'Coast Range Suture' is unspecific in comprising the entire contact zone all along the South Chilean coast, the term 'Linea de Purén' is misleading as the town of Purén is not located on the fault trace. From a tentative correlation of the fault zone with the similarly NW-SE striking dextral Jurassic Gastre Fault System (cf. Rapela & Pankhurst, 1992) in Central Patagonia, Argentina, it was termed 'Gastre Fault Zone' or 'Gastre-Purén Fault Zone'. However, in the present work we show that this correlation is incorrect. The lake 'Lago Lanalhue', in the western slopes of the Cordillera Nahuelbuta (Fig. 1) is located on the fault trace and shows a NW-SE-elongated shape. We therefore propose the new term *'Lanalhue Fault Zone (LFZ)'* as an appropriate name for the here discussed fault zone.

In this work, we present the first direct geochronological data for Lanalhue fault activity, combined with macro- and microstructural observations, to clarify evolution and geodynamic significance of the fault zone. New geochronological data on the regional basement units indicate that the activity of the LFZ initiated in Early Permian times, immediately after consolidation of the involved basement segments. Fluid inclusion data on fault-related quartz mineralizations help to constrain the post-metamorphic exhumation history. We present a new model on the assembly and subsequent segmentation of the Late Carboniferous to Triassic active continental margin in South Central Chile.

2. Geological setting

Along the Pacific coast of Central Chile, Late Paleozoic to Triassic processes assembled and shaped the southwestern margin of Gondwana (Hervé et al., 1987; Mpodozis & Ramos, 1989, Glodny et al., 2006). Whereas in northern Chile Late Paleozoic to Triassic structures are largely overprinted by the Andean orogeny in Jurassic to Recent times, the South Central Chilean margin shows abundant pre-Andean basement, preserved in a remarkably stable, stationary active margin setting. Below, we characterize the pre-Andean geologic units of a composite NE-SW profile across the LFZ, i.e, from the granitoids of the Cordillera Nahuelbuta into the Western Series paleoaccretionary forearc complex (Fig. 2).

The granitoids of the Cordillera Nahuelbuta (37°-38°S), as part of the Southern Coastal batholith of South-Central Chile, are calc-alkaline rocks, in particular granodiorites, tonalites, and diorites, with minor granites, intruded at upper crustal levels into metasedimentary sequences. Age determinations for these granitoids cluster tightly around 295-305 Ma (Hervé et al., 1988; Lucassen et al., 2004). The Nahuelbuta granitoids are remnants of a Late Carboniferous to Permian magmatic arc. While towards the north equivalents of the Nahuelbuta granitoids and their host rocks are found in the Coastal Cordillera, south of 38°30'S equivalents are located in the western flank of the Andean Main Cordillera, in the Lake District of South-Central Chile at ~40°S, east of Valdivia (Fig. 1). Here, magmatic arc rocks similarly intruded into metasediments and have been dated to between 316 and 285 Ma (Beck et al., 1991; Martin et al., 1999). Other Late Carboniferous intrusives are located in Argentina, close to the Chilean border, between 39° and 40° S (Varela et al., 1994; Lucassen et al., 2004, and references therein).

Eastern Series metasedimentary rocks, forming the host rocks of the Nahuelbuta intrusives, are characterized by pelitic-arenitic sequences, interpreted as continent-derived, mostly turbiditic successions (e.g., Hervé, 1988). Metabasites are absent in the here studied Central Chilean part of the Eastern Series. In the Cordillera Nahuelbuta area, the Eastern Series rocks form a belt along the western and southwestern flanks of the Nahuelbuta granitoids. Metamorphism is of high T / low P signature; the metamorphic grade is highly variable. In general, metamorphic grade increases towards the Nahuelbuta granitoids, from biotite grade through an andalusite zone towards a sillimanite zone in amphibolite-granulite facies (González-Bonorino & Aguirre, 1970; Hervé, 1977*).* A decrease in metamorphic grade is inferred for portions of the Eastern Series in immediate vicinity to the Lanalhue Fault Zone (Hervé 1977). For a low grade schist sample from the Concepción area, distant to the

Lanalhue Fault Zone, the age of metamorphism is constrained by K-Ar white mica fine fraction data to >298 +/- 8 Ma (Lucassen et al., 2004).

Locally preserved remnants of Eastern Series lithologies, which form the roof of the Nahuelbuta batholith, are mainly converted to high-grade, sillimanite-bearing gneisses and migmatites (cf. Hervé, 1977). In contrast, at some distance from both the LFZ and the granitoid intrusions (e.g., near the town of Lumaco, Fig. 2), weakly folded, sub-greenschist facies slates with well-preserved primary sedimentary features occur..

Similar metasedimentary successions are described, associated with the magmatic equivalents of the Nahuelbuta granitoids, in the Lake district (40°S). Here, turbiditic and siliciclastic metasediments previously known as part of the Panguipulli formation are now referred to as Trafún Sequence (Martin et al., 1999). Metamorphism is related in time and space to Late Carboniferous- Early Permian granitoid magmatism (Martin et al., 1997; 1999), and the rocks are attributed to the Eastern Series (Aguirre et al., 1972; Hervé et al., 1974; Martin et al., 1999). At ~40°S, Eastern Series rocks locally occur even within and east of the Andean Main Cordillera, partly in the roof zone of the Late Mesozoic to Cenozoic North Patagonian Batholith (Franzese, 1994; Rosenau, 2004) A phyllitic schist of this area, from east of Lago Pirihueico (at 40°S, a few kms from the Chilean border) yielded a Permo-Carboniferous Rb/Sr deformation age of 270 +/- 22 Ma (Rosenau, 2004). Further south, several other occurrences of metasediments resembling Eastern Series lithologies have been described within the Andean Main Cordillera, e.g., near Puerto Cisnes, 45°S (Levi et al., 1966; Aguirre et al., 1972). Isotopic age data on metamorphism are sparse. An age value of 292 ± 4 Ma was reported for low-grade metamorphic rocks surrounded by Cretaceous granitoids, east of Chiloé island at ~ 42°S (Pankhurst et al., 1992). Permo-Carboniferous metamorphism of turbidites, together with indications for a Permo-Carboniferous initiation of a magmatic arc, also characterizes the Eastern Andes Metamorphic Complex, Chile/Argentina at ~47° to 50°S (Hervé et al., 2003 and references therein).

Eastern Series successions have most probably been deposited on top of continental crust (Kato, 1976). For Eastern Series-equivalent rocks of both Central and Southern Chile, a

Devonian to Carboniferous passive margin depositional setting has been inferred (Hervé et al., 1987; Bahlburg & Hervé, 1997; Augustsson & Bahlburg, 2003). Structural observations in the Lake District (Chile, ~40°S) point to partly syndepositional early deformation of these Eastern Series rocks (Parada, 1975) which would imply sedimentation lasting until formation of an active margin setting in Late Carboniferous times (Willner et al., 2004, and references therein) and until incipient integration of these sediments into the backstop of the Carboniferous accretionary system (cf. Hervé et al., 1988).

Several Triassic basins with sedimentary and volcanosedimentary rocks, in places showing some compressional deformation (Martin et al., 1999), occur on top of the Paleozoic magmatic arc granitoids and the Eastern Series (Fig. 1), but are conspiciously absent on Western Series basement towards the southwest of the study area. The Triassic Galvarino basin (Fig. 2), located on Eastern Series basement only a few km north of the trace of the LFZ, is filled with continental siliciclastic detritus, possibly of granitic origin, as documented for the Triassic Panguipulli Formation of the Lake District, 40°S (Hervé et al., 1976). The lack of penetrative deformation in the sediments of the Galvarino basin points to a Triassic minimum age for the Lanalhue fault-related deformation (Kato, 1985). The NW-SE elongated shape of the Galvarino basin parallels the Lanalhue fault trace, but is also consistent with the general sense of strike of other Triassic basins further north in Central Chile and Argentina (Charrier, 1979). The abundant bimodal volcanic intercalations within the successions of many of the Triassic basins are evidence for important extension and rifting north of ~38°S in Triassic time (Franzese & Spalletti, 2001).

Western Series rocks form a belt all along the Chilean coast between 34°S and the island of Chiloé (42°S), with equivalents even further south, and consist of metasediment-metabasite intercalations. Main lithologies are meta-turbidites (metapelites, metapsammites), chlorite schists and minor metabasites, with local occurrences of ribbon cherts, serpentinites, and sulphide bodies. Geochemical signatures indicate similarity of the metabasites to ocean floor basalts (Hervé et al., 1988). The metamorphic signature of the Western Series implies a distinct high-pressure-low temperature, transitional greenschist- to blueschist facies imprint (Collao & Alfaro, 2000). Recorded maximum metamorphic conditions are in the range of 420°C, 8-9 kbar in most lithologies throughout the unit (Willner et al., 2001, and references therein; Glodny et al., 2005; Willner, 2005). Structurally, the Western Series complex is characterized by a dominant, mostly subhorizontal, near-penetrative transposition foliation, which is related to low angle recumbent nappe structures. This foliation is overprinted in places by folding and by zones of coplanar mylonitic shear (Glodny et al. 2005). Mineral stretching lineations and fold axes as well as compositional variations generally show a NW-SE trend (Kato, 1985; Godoy & Kato, 1990; Martin et al., 1999; Glodny et al., 2005). The complex has been shown, by reflection seismic imaging at 38°15'S (Krawczyk & the SPOC Team, 2003), to continue to depth, down to the present-day plate interface. As a whole, it constitutes an extinct forearc accretionary prism, assembled by basal accretion, which has been active in Late Paleozoic to Triassic time (Hervé, 1988; Martin et al., 1999; Glodny et al., 2005; Willner et al., 2005, Glodny et al., 2006). In the Valdivia area (~40°S) basal accretion and, in consequence, internal deformation of the Western Series ceased at about 200 Ma (Glodny et al., 2005).

3. The Lanalhue Fault Zone: structural and petrological observations

Fieldwork within and near the LFZ, in the area around Capitán Pastene and Lumaco (Fig. 2) revealed a refined image of fault characteristics and of structural features of the deformed country rock units.

Eastern Series lithologies, at a distance of several km from the Western Series-Eastern Series contact, not affected by fault movements, exhibit a mineral foliation S_1, with syn- to postkinematic growth of andalusite, biotite or staurolite porphyroblasts (Fig. 3a). Such late- to postkinematic porphyroblast growth has similarly been reported by Martin et al. (1999) and seems to be a regionally consistent feature. Eastern Series rocks show a steep metamorphic gradient with decrease in direction towards the fault contact, i.e. away from the granitoid batholiths (cf. Hervé, 1977). When approaching the LFZ, a few km away from the fault a crenulation cleavage / schistosity (S_2) appears and becomes more and more dominant, progressively leading to complete obliteration of sedimentary textures and of the primary S_1 mineral foliation near the contact. Close to the fault trace, S_1-S_2 is rotated towards fault-parallel NW-SE directions, and NW-SE oriented, generally horizontal mineral stretching lineation is frequently observed (Fig. 4; Burón, 2003; Ardiles, 2003). Microtextures, like occurrence of rotated and partly retrogressively transformed biotite, andalusite and staurolite porphyroblasts (Fig. 3b) suggest that this S_2 strain is *post*-peak-T with respect to the high-temperature metamorphism. Development of S_2 is kinematically linked to formation of discordant, quartz-dominated segregations with semibrittle to brittle fracture geometries (tension gashes, Fig. 3c). The abundance of tension gashes increases towards the fault zone. From deformation fabrics we estimate maximum temperatures in the range of 250 to 350 °C, i.e., near the brittle-ductile transition (cf. Stöckhert et al., 1999), during D_2 shearing in Eastern Series rocks close to the fault trace. This is consistent with the observed stability of biotite+chlorite assemblages. Late increments of deformation may have occurred at even lower temperatures as suggested by fault-related cataclasites.

The LFZ itself is detectable on satellite images as a regional lineament, and can be identified in the field as a several hundred meter wide, moderately E- to NE-dipping zone with abundant quartz mobilisates and intense plastic to brittle rock deformation. Senses of rotation of foliation planes, as well as mineral stretching lineations indicate a sinistral sense of shear (Fig. 4). Morphological contrasts across the LFZ, the occurrence of fault-controlled small Miocene sedimentary basins (Fig. 4), and the control of the LFZ on Quaternary sedimentation patterns (e.g., Rehak et al., 2008, and references therein) point to episodic minor Cenozoic fault reactivation.

In places the fault zone appears to be split into two or more subparallel branches. In outcrops, massive, up to m-thick hydrothermal quartz is frequently observed (Fig. 3d). This 'quartz anomaly' locally leaves a conspicious trace of quartz boulders in the mostly thick soils of the region. Formation of massive quartz mineralization was associated with brittle faulting, as evident from wall rock clasts of various sizes embedded into the quartz.

Within Western Series rocks, no distinct gradients in metamorphic grade or abundance of mineralizations are observed. The fairly consistent NW-SE trends of fold axes, mineral stretching lineations and flat-dipping, NW-SE striking foliation planes are developed throughout (Ardiles, 2003), near-parallel to the sense of strike of the LFZ. In contrast to tension gash occurrences within Eastern Series rocks, quartz mineralizations here are mainly oriented parallel to the foliation planes.

4. Sampling

To constrain the timing of specific deformation processes within the Western and Eastern Series as well as along the LFZ, different rocks were analyzed applying a tectonochronologic approach..Detailed descriptions of the samples are given in the Appendix.

For direct dating of deformation along the Lanalhue Fault Zone, we investigated tension gash mineralizations developed within Eastern Series rocks (see Fig. 2; samples VAL64 and VAL65, the latter enclosed by schist of sample VAL65S; sample VAL64 was collected southeast of Capitán Pastene, sample VAL65 is from between Capitán Pastene and Lumaco). Late increments of faulting are recorded by sample VAL63 (collected 15 km NW of Capitán Pastene) which is from a massive quartz mineralization within the fault trace.

Two samples of Western Series schists of the Lago Lanalhue region (samples VAL62, LAH1, Fig. 2) have been investigated, to date the end of the main ductile deformation in these rocks (cf. Glodny et al., 2005). To constrain late stages of deformation within the Western Series, related to the waning of progressive basal accretion, we sampled material from a structurally late, semiductile shear band at Tirúa, Pacific coast at 38°20'S (sample VAL61) which cuts the main foliation of the surrounding schist.

Eastern Series lithologies have been collected both in the vicinity of the Lanalhue fault trace (sample VAL65S, structurally overprinted by Lanalhue fault related deformation), and at Playa Chivilingo (Pacific coast at 37°09'S, Fig. 2). Playa Chivilingo is located close to the inferred contact of the Eastern Series to Western Series rocks further west (cf. Hervé, 1977). Here, texture analysis reveals two successive foliations, S_2 being later and dominant. S_2 surfaces are axial-planar in thin section and outcrop scale. In contrast, S_1 surfaces are folded, as evident from thin, S_1-parallel, folded and offset quartz veinlets (cf. Hervé, 1977). In places, up to meter-sized metamorphic mobilisates occur, which we interpret as prograde-metamorphic, dehydration-related features. Field evidence suggests that formation of these mobilisates occurred prior to at least the last increments of S_2, because the foliation in the enclosing schists is bent around mobilisate masses. Both the mobilisate (sample VAL60a, Fig. 3e) and the enclosing schist were analyzed (sample VAL60c, Fig. 3f).

We also dated two samples of Cordillera Nahuelbuta granitoids (FLO1, ANG1), and a migmatitic gneiss sample from the roof zone of the Cordillera Nahuelbuta batholith (sample NPN2), to correlate Eastern Series deformation with the peak of the thermal overprint.

5. Analytical methods

For isotopic dating we used the Rb/Sr internal mineral isochron approach. Small samples (~20-100 g) have been choosen which clearly relate to specific increments of the structural and metamorphic evolution and show a minimum of subsequent overprint. The Rb/Sr system of white mica, the phase on which most of our age data is based, is thermally stable to temperatures >500°C but may be reset by dynamic recrystallization (von Blanckenburg et al., 1989; Freeman et al., 1997; Villa, 1998). This ensures dating of either assemblage crystallization or of deformation processes in most of our samples (cf. Glodny et al., 2005). We generally tried to check for isotopic equilibrium relationships within a rock by analyzing as many different Sr-bearing phases as possible. To check for possible Sr-isotopic inhomogeneities resulting from long-term incomplete dynamic recrystallization, diffusional Sr redistribution and/or alteration processes, white mica was usually analyzed in several, physically different (by magnetic properties and/or grain size) fractions. All mineral concentrates were checked and finally purified by hand-picking under a binocular microscope. Quartz separates were further treated with cold (20°C) concentrated hydrofluoric acid for ~30 seconds in an ultrasonic bath, to remove surface contaminants.

Rb and Sr concentrations were determined by isotope dilution using mixed ^{87}Rb-^{84}Sr spikes. Determinations of Rb and Sr isotope ratios were carried out on a VG Sector 54 TIMS instrument (GeoForschungsZentrum Potsdam). Sr was analyzed in dynamic multicollection mode. The value obtained for ^{87}Sr/^{86}Sr of the NBS standard SRM 987 was 0.710268 ± 0.000015 (n = 19). The observed ratios of Rb analyses were corrected for 0.25% per a.m.u. mass fractionation. Total procedural blanks were consistently below 0.15 ng for both Rb and Sr. Due to highly variable blank values, no useful blank correction was applicable. Isochron parameters were calculated using the Isoplot/Ex program (Ludwig, 1999). Standard errors, as derived from replicate analyses of spiked white mica samples, of +/- 0.005% for ^{87}Sr/^{86}Sr ratios and of +/- 1.5 % for Rb/Sr ratios were applied in isochron age calculations (cf. Kullerud 1991). Individual analytical errors were generally smaller than these values.

Fluid inclusion analyses on coarse-grained quartz from fault-related mineralizations have been realized in the microthermometry laboratory at the Departamento de Ciencias de la Tierra, Universidad de Concepción, Chile, using a Linkam TH-600 heating and freezing stage. Methodology is described in Shepherd (1981).

6. Results

6.1. Rb-Sr data

Rb/Sr results are presented in Tab. 1. Fig. 5 shows isochron plots for samples associated with the activity of the Lanalhue Fault Zone. For fault-related quartz mobilisates, from both the fault trace and from two different tension gashes, age values between 271.6 and 280.3 Ma are obtained, all identical within limits of error. A similar age value is found for a sample of Lanalhue-deformed Eastern Series schists (274 +/- 12 Ma, sample VAL65S).

Two samples of Western Series schists, collected at a distance of ~15 km from the fault trace and ~20 km apart from each other (Fig. 2) give contrasting results. While the age obtained from VAL 62 (272.7 +/- 2.8 Ma) is comparable to the age of Lanalhue fault activity, sample

LAH3 yields an age value of 294.3 +/- 9.4 Ma. The structurally late shear band from Tirúa yields an age value of 255.8 ± 2.7 Ma.

Eastern Series rocks from Playa Chivilingo consistently show Rb/Sr mineral ages around 295 Ma, both for the prograde mobilisate and for late increments of deformation. Ages around 295 Ma are similarly determined for Eastern Series-equivalent high-grade metamorphic rocks from the Cordillera Nahuelbuta (sample NPN2, 297.3 +/- 2.5 Ma). Ages of 286.3 +/- 4.2 Ma (biotite-feldspar age, ANG1) and 306.8 +/- 4.5 Ma (granitic pegmatite, FLO1) result for the intrusive igneous rocks of the Cordillera Nahuelbuta.

6.2 Microthermometric data

Quartz samples from the fault mineralization (sample VAL63) and from a tension gash fill (VAL64) show abundant fluid inclusions. Inclusions consist of fluid + vapor, are fluid-rich (generally 85-90% fluid by volume; some gas-dominated inclusions are present in sample VAL63), and have densities between 0.8 and 1.0 g/cm^3. Solid precipitates were not observed. No significant physico-chemical differences were detected between primary, pseudosecondary, and secondary fluid inclusions. Analytical data are presented in Tab. 2. Mean fluid inclusion homogenization temperatures for both samples are identical within limits of error (154.4 +/- 43.0 °C and 171.5 +/- 47.8 °C for the fault mineralization and the tension gash quartz, respectively).

7. Discussion

7.1 Interpretation of age data

Lanalhue fault – related quartz mineralizations give Rb/Sr mineral ages between 272 and 280 Ma. These ages are calculated using data for fine-grained muscovite, which is very rare within the mineralizations, but occasionally present forming small 'nests' or planar enrichment zones possibly resembling former fractures or fluid pathways. Other accessories within the mineralizations are albitic feldspar and chlorite. The host rocks of the quartz mineralizations are characterized by occurrence of abundant graphite, present as inclusions in nearly all mineral phases. Complete absence of graphite from the mineralization indicates that muscovite, chlorite and feldspar are co-genetic with the bulk quartz and do not represent entrained wallrock material. We therefore interpret the above ages as assemblage crystallization ages. The formation of the studied, structurally late mineralizations may have been a polystage process, as evident from the inhomogeneous distribution of accessory phases within the quartz as well as from the low but variable degree of brittle deformation recorded by the quartz. Polystage mineralization or overprint by late fluid infiltration may also be inferred for the inconsistency between the Rb/Sr isotopic results for two analyzed quartz fragments from sample VAL64, which leads to a high MSWD value for regression and to a comparatively high age error (Tab. 1). The age value obtained from the host rock of one tension gash (274 +/- 12 Ma, sample VAL65S) is interpreted as a deformation age. Although imprecise, it is additional evidence for Early Permian (~275 Ma) formation of the deformation fabrics and mineralizations associated with late increments of deformation along the Lanalhue Fault Zone. These results show that there is no tectonic link between the LFZ and the Jurassic Gastre Fault Zone (*sensu* Rapela & Pankhurst, 1992) of Argentina. Major post-Permian movements along the LFZ, as previously inferred or suggested, can be ruled out.

Fluid inclusion data show that quartz mineralizations were formed at low temperatures, at around 150-200°C. Because granitic igneous rocks and hydrothermally active fault systems are commonly characterized by elevated near-surface geothermal gradients relative to their surroundings, we infer very low pressure conditions during formation of the mineralizations. This implies that regional exhumation to near-surface depths (< 5 km) of at least the fault rocks and adjacent Eastern Series lithologies and Late Paleozoic arc intrusives was already completed in Early Permian times. There have been no major vertical displacements or erosional episodes in the immediate LFZ region or north and east of it after ~275 Ma that exceeded a few km. This is corroborated by nearby presence of Triassic sediments on top of Eastern Series and granitoid basement, as well as by results of zircon fission track dating in the area (Glodny et al., 2008). Minor Cenozoic fault reactivation, with brittle movements of minor (≤1 km) vertical amplitudes is inferred from the presence of local Miocene basins along the fault trace (Fig. 4).

Granitoids of the Late Paleozoic arc in the Cordillera Nahuelbuta apparently intruded in a short time interval between ~310 to 285 Ma (Late Carboniferous to Early Permian). This range of ages has previously been established for both Cordillera Nahuelbuta and Lake Region granitoids (Hervé et al., 1988; Martin et al., 1999; Lucassen et al., 2004, and references therein). Our new results are compatible with this age interval. The biotite-feldspar age of sample ANG1 (286.3 ± 4.2 Ma) is best interpreted as a minimum age for crystallization, and may be very close to the crystallization age, as the degree of postmagmatic alteration is very low in this rock. The muscovite age from the coarse grained granitic pegmatite sample FLO1 (306.8. ± 4.5 Ma) is interpreted as a true crystallization age, because the Rb-Sr system in pegmatitic white mica is extremely robust against overprints (cf. Glodny et al., 1998). It dates the latest stage of local granitoid crystallization, in a supracrustal level. The age is, within limits of error, identical to Rb/Sr and Sm/Nd mineral isochron ages for nearby igneous or anatectic rocks (306 ± 6 Ma and 308 ± 7 Ma, Lucassen et al., 2004).

Eastern Series rocks, both at Playa Chivilingo (samples VAL60a, VAL60c) and in the roof zone of the Cordillera Nahuelbuta granitoids (migmatitic sample NPN2) yield ages of ~295-300 Ma (Tab. 2). The age result for sample NPN2 is based on biotite, white mica and feldspar, i.e., on phases with different closure temperatures for intracrystalline diffusion. Nevertheless, a statistically valid isochron (sensu Kullerud, 1991) has been obtained. We interpret the age value of 297.3 +/-2.5 Ma as an assemblage crystallization age, equivalent to the age of peak thermal overprint of this rock. This interpretation is compatible with the age data obtained for the Eastern Series mobilisate at Playa Chivilingo. Although the age value for the mobilisate is less precise (sample VAL60a, 295 ± 14 Ma) textural evidence shows that it formed prior to the last increments of ductile deformation (Fig. 3e,f) which are dated at

294.8 ± 3.4 Ma (sample VAL60c, Tab. 2). At Playa Chivilingo, both prograde mobilisate formation and ductile deformation were nearly completed at ~295 Ma. This age value is identical to K-Ar data for white mica from Eastern Series schists near Concepción (isotopic closure at ≥ 298 ± 8 Ma, Lucassen et al., 2004), and to K-Ar-based age data for similar schists further north, at ~35°S (Willner et al., 2005) In summary, these ages show that the thermal evolution of Eastern Series lithologies distal to the LFZ was near-contemporaneous and most probably genetically linked to the intrusion of arc granitoids in a convergent margin setting. The observation of pre-S_2 staurolite and biotite and syn- to post-S_2 andalusite and garnet (Hervé, 1977) suggests, in line with previous inferences by Kato (1976), that the thermal overprint was syn- to late D_2 in the area.

Western Series rocks south of the LFZ yield isotopic ages documenting a prolonged history of structural and metamorphic evolution. Our age data for schists, interpreted as dating the waning stages of synkinematic recrystallization and ductile deformation (cf. Glodny et al., 2005) define the establishment of the now visible, high-pressure greenschist facies metamorphic and structural signature at 272.7 ± 2.8 Ma (sample VAL62) and 294.3 ± 9.4 Ma (sample LAH3). With its age value of 255.8 ± 2.7 Ma, the structurally late, semiductile shear zone from Cabo Tirúa points to ongoing deformation within the Western Series at least until Late Permian times. Within the regional context, these age values are complemented by a K-Ar age of 282 +/- 6 Ma for a Cr-bearing white mica from La Cabana (38°32'S, 73°18'W, about halfway between Tirúa and Temuco, Fig. 2), interpreted as dating a late stage of ductile deformation (Höfer et al., 2001). In the Tirúa area, several ages for the main penetrative deformation cluster around 285 Ma, while tension gashes, constituting the youngest isotopically datable stage of the structural evolution, formed at ~252 Ma at upper crustal levels in the brittle regime (Glodny et al., 2006).

In the Valdivia area (39°45'S, Fig. 1), Western Series rocks show a metamorphic and structural evolution which is strikingly similar to the here studied region and has been interpreted as reflecting basal accretion in a forearc wedge setting (Glodny et al., 2005).

While the main deformation of the schists is related to processes during or immediately after basal accretion, formation of semiductile shear bands and tension gashes is interpreted to result from progressive deformation at higher crustal levels, related to antiformal stacking above the site of tectonic underplating (Glodny et al., 2005). The only significant contrast between the evolution of Western Series rocks in the study area and near Valdivia is the higher absolute age of the end of accretion, with ~252 Ma immediately near the LFZ vs. ~ 200 Ma near Valdivia.

7.2 Geodynamic implications

7.2.1. Wedge architecture

The nature of the contact between the Western and Eastern Series has been a matter of continuous debate. The contact is of continental dimension, with continuous presence of both Western and Eastern Series rocks for considerably more than 1000 km along the continental margin of Central and Southern Chile. Across the contact, there are consistent changes in lithology and metamorphic signature. Therefore, it seems clear that at a comparatively early stage of its evolution the contact has been a genetically and structurally homogeneous feature. However, the contact appears to be overprinted in different ways along strike. As shown here, in the Lanalhue Fault segment, last movements were characteristic for a sinistral ductile to brittle transform fault. Immediately north of Lago Lanalhue, the contact was reactivated in Cenozoic time as a fault with large vertical displacement (Hervé, 1977). While north of about 37°S it has in parts been described as transitional (González-Bonorino, 1971, Richter et al. 2007), between 34° and 35°S the contact in places cuts metamorphic isograds within the Eastern Series and appears as a Cretaceous(?) brittle reverse fault (Pichilemu-Vichuquén fault; Willner et al., 2005).

Forearc accretionary wedges may be built by principally two modes of accretion, namely basal and frontal accretion (e.g., Moore & Silver, 1987; Gutscher et al., 1998). The Western Series has all characteristics of a basally accreted wedge domain, like metabasite intercalations originating from the subducting oceanic plate, duplex/nappe structures, and a pronounced HP/LT signature (Willner et al., 2000; Willner, 2005; Glodny et al., 2005). The Eastern Series shows a structural inventory similar to that of the Western Series, indicative of deformation similarly within an accretionary wedge setting. However, the Eastern Series has no high P/ low T metamorphic imprint and is devoid of metabasitic lower plate components. Its tectonic and lithologic signature is characteristic for frontally accreted material (e.g., Lohrmann, 2002, Richter et al., 2007), indicating that the Eastern Series was built by accretion of pre-subduction passive margin slope sediments. Consequently, the Eastern Series has been considered as to represent a unit located in the rear of the wedge, in a position transitional to the backstop system (Hervé, 1988; Willner et al., 2000). We infer that the Western and Eastern Series represent genetically different structural units of one and the same Late Paleozoic active continental margin accretion complex. The difference between these units is in the mode of wedge growth, with frontal accretion of exclusively siliciclastic, continent-derived passive margin sediments in the Eastern Series, and basal underplating of subduction-related plate boundary material in the Western Series. Isotopic age data support this inference, as the onset of buildup of the subduction-accretion system in South Central Chile is constrained by peculiar Western Series rocks (garnet amphibolites from Los Pabilos, Coastal Cordillera at ~41°S) to slightly earlier than 305 Ma (Kato & Godoy, 1995; Willner et al., 2004). This is very close in time to the here presented age data for both magmatic arc igneous activity and Eastern Series fold and thrust belt deformation. It appears that only about 10 Ma elapsed between onset of Eastern Series fold-and-thrust belt deformation (triggered by initiation of subduction) and its termination after intrusion of arc granitoids.

7.2.2. Model of margin evolution

In the following we develop a conceptual model for margin evolution in South Central Chile, from incipient subduction to establishment of the LFZ. Considering the available structural, petrologic and geochronologic information, we suggest that initially the Western Series - Eastern Series association was formed during the early stages of subduction, in Late

Carboniferous time. In an initial stage, soon after initiation of subduction, folding and frontal duplexing of thick passive margin sediments caused incipient internal deformation of what is now the Eastern Series (Fig. 6a). Later on, underthrusting and basal accretion, processes which may occur concurrently and alternating with frontal accretion at one and the same margin (Gutscher et al., 1998) led to development of the Western Series as a basally accreted duplex complex (Fig. 6a,b). Synchronous to the formation of the accretionary complex, a pulse of magmatic arc magmas intruded syntectonically into the Eastern Series in the rear of the accretion system. Geochemical and isotopic evidence shows that arc intrusives carry a high proportion of reworked old crustal material (Lucassen et al., 2004), indicating that either the magmas assimilated large amounts of Eastern Series schists (which represent reworked old continental basement, cf. Lucassen et al., 2004; Glodny et al., 2006) or, more likely, that the Eastern Series was underlain by old continental basement (Fig. 6b).

Taking into account the time constraints for incipient subduction (slightly older than 305 Ma, Willner et al., 2004), for establishment of a basally accreted complex (oldest ages for HP greenschist facies deformation, between 300 and 290 Ma; Willner et al., 2005 and the present study) and for arc magmatism as outlined above, there was only a narrow time frame of less than ~20 Ma [~310-290 Ma) for full establishment of an accretive active continental margin. At ~290 Ma the Eastern Series was consolidated, and waning arc magmatism was coeval with still ongoing basal accretion in the Western Series. The contact between Western and Eastern Series at that time most likely has been a major N-S trending, E-dipping normal fault zone, in the eastern flank of the continuously upwarping Western Series (Fig. 6c). Such a geometry is suggested particularly by the shape of evolving basally accretive complexes in sandbox models (cf. Lohrmann, 2002; Glodny et al., 2005). Further, the dip of the contact towards east persists until today (Ardiles, 2003; Burón, 2003; Fig. 4). Kato (1976, 1985) reports observations of Eastern Series fragments entrained within Western Series rocks in the vicinity of the LFZ. This is similarly consistent with an early evolutionary stage of the presently exposed LFZ as a transtensional fault zone in the ductile regime between frontally and basally accreted parts of the wedge. It also indicates that in its early stages the Western

Series - Eastern Series contact probably was a deformation zone with transitional character and considerable width (up to a few km; Richter et al., 2007) Transtensional differential exhumation across the Western Series-Eastern Series contact is further inferred from P,T conditions of metamorphism and granitoid crystallization. Overall exhumation of both the Eastern Series and magmatic arc intrusives was minor, as evidenced by the pronounced low-pressure signature of metamorphism and the only exceptional occurrence of magmatic muscovite in the arc granitoids, whereas Western Series lithologies obtained their main structural imprint at crustal depths of more than 30 km.

An important observation along strike of the Chilean continental margin is the distance between the present day trench, and the western limit of the Late Carboniferous magmatic arc as given by its westernmost intrusive contact with Eastern Series rocks. While this distance is nearly constant at about 120 to 140 km north of 37°50°S, it amounts to ~230 km south of 39°40', in the Chilean Lake district where this intrusive contact is exposed again (estimates based on Bangs & Cande, 1997; SERNAGEOMIN, 2003). Given the fact that the modern accretionary complex is small and that Paleozoic-Early Mesozoic basement appears to be present at only 20-30 km east of the trench line (Bangs & Cande, 1997), there is a marked longitudinal change in the width of the preserved Late Paleozoic-Early Mesozoic forearc system. Within the only ~200 km continental margin segment between 37°50'S and 39°40'S, this width changes from ~100 km (N) to nearly 200 km (S). The western limit of Paleozoic arc granitoids, found in the western flank of the Coastal Cordillera in the north, is located within the Andean foothills further south (Fig. 1). The contact between Western Series and Eastern Series rocks is, from map evidence, inferred to be shifted in the same way in its position relative to the trench, with a sinistral offset of ~100 km.

As the two distinct width domains of the Paleozoic-Early Mesozoic forearc are connected by the sinistral LFZ (Fig. 6d), it seems likely that the evolution of the above forearc width contrast is genetically linked to fault activity, i.e., that the Paleozoic magmatic arc is dissected and displaced along the NW-SE striking Lanalhue fault system for nearly 100 km relative to the present day trench. A key observation supporting margin dissection is that the axis of the Carboniferous magmatic arc is, by the Lanalhue Fault Zone, directly iuxtaposed with Western Series rocks - which were formed in an entirely different setting. Therefore, the Lanalhue Fault Zone cannot reflect an original curvature of the continental margin. A previously suggested transcontinental, NW-SE trending shear zone as a possible reason for this margin dissection seems unlikely as hypothetically Lanalhue-correlated strike-slip structures in Argentina are either dextral, Mesozoic in age, or entirely disputable (Rapela & Pankhurst, 1992; von Gosen & Loske, 2004). The reason for margin dissection may thus be found within the evolving active margin system itself. Active margins are known to behave in different ways. Distinction is made between accretive, non-accretive, and tectonically erosive margins, the latter with significant losses of continental material (von Huene & Scholl, 1991; von Huene & Ranero, 2003). Margin behaviour with respect to accretion/erosion may change with time as well as along strike, mainly in response to the availability of trench fill sediment, but also in response to spreading ridge subduction (Bangs & Cande, 1997; Behrmann & Kopf, 2001, and references therein).

In Northern Chile, appearance of Mesozoic magmatic arc rocks in coastal cliffs, together with a distance of only ~100 km between these and the trench has been taken as evidence for subduction erosion (v. Huene & Ranero, 2003). In South Central Chile, north of 37°50', Late Paleozoic intrusive rocks are located at distances of ~130 km from the present day trench – which is still considerably less than the characteristic arc-trench distances for todays active margin systems. Furthermore, south of the LFZ the Paleozoic magmatic arc nearly coincides with the present-day arc, whereas north of the LFZ the Paleozoic arc is displaced towards the trench for nearly 100 km relative to the present day arc position. Thus, the Late Paleozoic forearc structure appears to be truncated in the region north of the LFZ, with significant mass loss of the western parts of the Western Series. In contrast, to the south of the present LFZ, the continental margin was continuously accretive during the Permian, i.e., during the period of formation of the LFZ (see also Glodny et al., 2005, 2006). Such a scenario of differential margin evolution along strike should establish tectonic forces in response to the differential stress regimes imposed on the upper plate, capable of reactivating the former normal fault contact between Western and Eastern Series with a now predominant sinistral strike-slip component. Truncation of the margin structure with selective mass removal north of 38°S may also be achieved by northward trench-parallel translation of outer forearc material along hypothetic dextral, trench-parallel shear zones, as proposed for Early Mesozoic times (Martin et al., 1999). However, to the best of our knowledge, unequivocal evidence of coherently displaced Western Series slices north of 36°S is lacking. Admittedly, this does not mean that displaced Western Series rocks has never been there - they could have been removed by post-mid Jurassic tectonic erosion (e.g., von Huene & Ranero, 2003)

We therefore suggest that the differential margin behaviour is due to pronounced accretion in the south, most likely contrasting with tectonic erosion north of ~38°S. This differential behaviour dates back to the Early Permian, to the period of the sinistral, semibrittle to brittle overprint of the contact between Western and Eastern Series (Fig. 6d) that led to establishment of the present structural architecture of the LFZ. The new geochronologic data for fault mineralizations and tension gashes date late stages of brittle strike-slip faulting to roughly between 280 and 270 Ma. However, because these data relate only to the late increments of deformation, initiation of the LFZ as a sinistral strike-slip fault may have commenced earlier, possibly as early as close to 300 Ma, immediately after the waning of internal deformation of the Eastern Series. Assuming activity of the LFZ for ~30 Ma, an average rate of sinistral slip along the LFZ in the range of ~3 km/Ma can be estimated. Assuming that this slip rate is entirely due to tectonic erosion N of the the LFZ, such a rate appears plausible as it is well within the range of published tectonic erosion rates for Cenozoic continental margins (Clift & Vannucci, 2004, and references therein). A modern analogy to the proposed Late Paleozoic margin evolution is possibly found in Central Chile (33°S). Here, the Juan Fernández ridge is subducted, in a position which did not change much in the last 10 Ma (Yáñez et al., 2001). The ridge separates a sediment-starved trench in the north, with predominant tectonic erosion of the continental margin, from a sediment-filled trench in the south, with margin behavior fluctuating between accretion and nonaccretion/tectonic erosion (Bangs & Cande, 1997; von Huene et al., 1997; Yáñez et al., 2001), which results in marked contrasts in tectonic forearc-arc evolution. Tectonic erosion in central Chile north of the Juan Fernández ridge collision point amounts to >30 km just within the last 10 Ma (Laursen et al., 2002), while accretion appears to dominate immediately south of the ridge intersection. In analogy to the inferences made for the development of the Lanalhue Fault Zone, this differential margin behaviour should generate an array of neotectonic forearc structures comprising major left-lateral strike-slip faults. In fact, a set of prominent, mostly sinistral and NW-SE trending shear zones is observed onshore near the ridge intersection point (Yáñez et al., 2001; SERNAGEOMIN, 2003) which we speculate to partly account for the dissection of the regional Jurassic magmatic belt and the trenchward displacement of its segment north of ~33°S, just in the same style as inferred for the Permian LFZ further south.

8. Conclusions

The Lanalhue Fault Zone is a Permian crustal-scale strike-slip fault with a complex evolution. It initially evolved from a large scale, NNE-SSW trending normal fault zone within the forearc accretionary complex. In its early stages, in Late Carboniferous times, this fault zone separated the basally growing, continuously upwarping and exhuming Western Series in the west from frontally accreted former slope sediments further east. Later on, in the Early Permian (>280-270 Ma), a specific segment of the Western Series-Eastern Series fault contact between 37°50’S and 39°45’S was reactivated and transformed into a sinistral, semiductile to brittle strike slip fault. This fault dissected the established active margin architecture and displaced forearc zonation patterns, like the western front of Late Paleozoic arc intrusives, for nearly 100 km relative to the trench line. Fault movements of this stage are inferred to relate to Early Permian differential margin evolution north and south of about 38°S, with ongoing accretion in the south, and tectonic erosion affecting the western flank of the Western Series in the north. Structural observations and fluid inclusion data indicate that fault activity continued during exhumation of the fault rocks through the ductile-brittle transition, and ceased when todays surface rocks had reached the ~150°C paleotemperature level. Exhumation of fault rocks and of the neighboring Eastern Series, which postdated the last documented fault movements (~270 Ma) thus was, assuming average upper crustal thermal gradients, less than ~3-4 km in total. Despite continuation of basal accretion and exhumation in the Western Series south of the LFZ until the Triassic, the LFZ itself did not accommodate any major post-Permian fault movements. The LFZ thus separates segments of the Late Paleozoic to Late Triassic paleomargin, defined by differential accretive and denudation histories. The Early Permian overprint and final shaping of the margin architecture persists until today, expressed in contrasting widths of the Western Series belt and in contrasting lithologies in the present Andean forearc region north and south of the Lanalhue Fault.

Acknowledgements

We thank J. Herwig, G. Arnold, V. Kuntz and M. Dziggel for their help with sample preparation and figure drawing, and all individuals from the Concepción geoscience community and the Berlin-Potsdam SFB 267 group who supported this work by various means. Careful and constructive reviews by A. Willner and T. Kato are gratefully acknowledged.

APPENDIX: SAMPLE CHARACTERIZATION

a) Quartz mineralization, Lanalhue Fault Zone

VAL63 (38°10.732' S, 73°04.584' W; roadcut 8 km WNW Capitán Pastene). Extensive quartz mineralization, massive or as near-vertically oriented, discordant "walls", apparently within the fault zone. Sample forms part of a 10 –100 m wide "quartz anomaly". Assemblage: Near-monomineralic quartz, locally with traces of $Fe(OH)_x$, sericite and chlorite.

b) Tension gashes (related to S_2), Lanalhue Fault Zone

VAL65 (38°11.483' S, 72°57.951' W; road between Cap. Pastene and Lumaco, 3 km from Cap. Pastene). Late, discordant tension gash in "Eastern Series" rocks, mineralized with quartz, oriented almost vertical, N-S. System of tension gashes associated with development of S_2 foliation. Assemblage: Almost monomineralic quartz, with traces of feldspar, white mica and chlorite. Matrix: see sample VAL65S.

VAL64 (38°16.972' S, 72°53.621' W; roadcut of small W-E road crossing the valley of Rio Lumaco, 13.5 km S of Lumaco). Vertical-discordant, quartz-dominated veins and tension gashes, cutting a megaboudin / anticlinal structure within the Eastern Series. N-S orientation of the quartz veins, in line with regional LFZ-related crenulation cleavage.

c) Eastern Series, influenced by Lanalhue Fault activity

VAL65S (38°11.483' S, 72°57.951' W; road between Cap. Pastene and Lumaco). Eastern Series. Fine-grained pelitic schist, very rich in carbon (graphite). Material forms the matrix for the quartz mineralization of sample VAL 65. Mineral association: blasts of amphibole, staurolite, chlorite and biotite in a fine-grained matrix of sheet silicates and quartz. Staurolite growth was prior to last increments of deformation; it also shows retrogression phenomena (chloritization / sericitization along rims and cracks).

d) Western Series, near the Lanalhue Fault Zone

VAL62 (38°13.627' S, 73°14.904' W; abandoned iron mining site "Mineral Mahuilque", 8 km NW' Relun). Western Series: strongly foliated albite-chlorite schist, intercalated with metachert. Assemblage: albite, quartz (partly recrystallized), chlorite/biotite, white mica, titanite, pyrite, epidote (rare).

LAH3 (38°02.971' S, 73°20.157' W; roadcut, ~6 km E of Antiquina). Western Series: garnet micaschist with quartz-dominated mobilisates. Assemblage: quartz, white mica, plagioclase, garnet, biotite/chlorite (rare), tourmaline, apatite (very rare)

VAL61 (38°20.544' S, 73°30.081' W, Cabo Tirúa). Semiductile extensional shear zone in micaschist. Shear zone was pathway for syndeformational fluid migration (associated with small quartz mobilisates). Material is strongly weathered. Assemblage: quartz, white mica, albite, chlorite, zircon (small, rounded), tourmaline, anatase.

e) Eastern Series, Playa Chivilingo

VAL60a (37°09.178' S, 73°11.031' W; southern end of Playa Chivilingo). Hydrothermal, coarse-grained, mostly quartz-dominated complex mineralization, forming semi-discordant, m-sized masses within quartzitic to chloritic schists. Mineralization was prior to last increments of deformation. Assemblage: quartz, clinozoisite, feldspar, muscovite, paragonite, wollastonite; traces of garnet, phlogopite, several unidentified trace phases.

VAL60c (37°09.178' S, 73°11.031' W; southern end of Playa Chivilingo, matrix of sample VAL 60 a). Chlorite-sericite schist with strong foliation. Assemblage: white mica, chlorite, feldspar, green amphibole, quartz, garnet.

f) Magmatic and migmatic rocks, Cordillera Nahuelbuta

FLO1 (36°46.515' S, 72°48.787' W; Road from Concepción to Florida, Bridge #6, Loc. Poñen) Granitic pegmatite. Gradual contact to granite, late magmatc stage. In places development of "graphic granite". No deformation. Assemblage: plagioclase, K-feldspar, quartz, white mica, biotite, garnet, zircon, monazite.

NPN2 (37°48.5’ S, 73°02.7’ W*)* Roadcut, 2 km SW’ Piedra de Aguila, Parque Nacional Nahuelbuta). Muscovite-rich migmatitic paragneiss, apparently forming a raft in granites. Assemblage: feldspar, quartz, muscovite, biotite, sillimanite, apatite, zircon, monazite, ilmenite, garnet.

ANG1 (37°49.6' S, 72°53.8' W; road between Angol and Parque Nacional Nahuelbuta, near Vegas Blancas). Granitoid. Assemblage: feldspar, quartz, biotite, amphibole, apatite (abundant), clinopyroxene, zircon.

References

Aguirre Le-Bert, L., Hervé, F., Godoy, E., 1972. Distribution of metamorphic facies in Chile - An outline. Krystalinikum 9, 7-19.

Ardiles M., 2003. La Serie Occidental del basamento metamórfico, centro sur de la Cordillera de Nahuelbuta, Chile, área Quidico-Capitán Pastene. Petrografía, mesoestructura y análisis microtectónico. Memoria de titulo, Dept. de Ciencias de la Tierra, Universidad de Concepción, Chile, pp. 1-132.

Augustsson, C., Bahlburg, H., 2003. Active or passive continental margin? Geochemical and Nd isotope constraints of metasediments in the backstop of a pre-Andean accretionary wedge in southernmost Chile (46°30'-48°30'S). In McCann T, Saintot A (eds) Tracing tectonoc deformation using the sedimentary record. Geological Society, London, Special Publications 208, 253-268.

Bahlburg, H., Hervé, F., 1997. Geodynamic evolution and tectonostratigraphic terranes of northwestern Argentina and northern Chile. Geological Society of American Bulletin 109, 869-884.

Bangs, N.L., Cande, S.C., 1997. Episodic development of a convergent margin inferred from structures and processes along the southern Chile margin. Tectonics 16, 489-503.

Beck, M.E.Jr., Garcia, R. A., Burmester, R.F., Munizaga, F., Hervé, F., Drake, R.E., 1991. Paleomagnetism and geochronology of late Paleozoic grantitic rocks from the Lake District of southern Chile: implications for accretionary tectonics. Geology 19, 332-335.

Behrmann, J.H., Kopf, A., 2001. Balance of tectonically accreted and subducted sediment at the Chile Triple Junction. International Journal of Earth Sciences 90(4), 753-768. DOI: 10.1007/s005310000172

Burón P., 2003. Petrografía, estructuras y microtectónica del área de contacto entre las series metamórficas del basamento Paleozoico entre los 38°08' y 38°21'S, Cordillera de Nahuelbuta, Chile. Memoria de titulo, Dept. de Ciencias de la Tierra, Universidad de Concepción, Chile, pp. 1-144.

Charrier, R., 1979. El Triásico en Chile y regiones adyacentes de Argentina: una reconstrucción paleogeografica y paleoclimatica. Comunicaciones, Universidad de Chile, Departamento de Geología, No 26, pp. 1-37, Santiago de Chile.

Clift, P., Vannucchi, P., 2004. Controls on tectonic accretion versus erosion in subduction zones: implications for the origin and recycling of the continental crust. Review of Geophysics 42, RG2001, doi:10.1029/2003RG000127.

Collao, R., Alfaro, G., 2000. Paleozoic massive sulphide orebodies of the Nahuelbuta and Queule mountains, South-Central Chile: results of geobarometry and sulphur isotope studies, in: R. Sherlock, M.A.V. Logan (Eds.), VMS deposits of Latin America, Geol. Association of Canada, Spec. Pub. 2, pp. 629-641.

Davidson, J., Mpodozis, C., Godoy, E., Hervé, F., Pankhurst, R.J., Brook, M., 1987. Late accretionary complexes on the Gondwana margin of southern Chile: evidence from the Chonos Archipelago. In: McKenzie, G.D. (ed.) Gondwana Six: Structure, Tectonics and Geophysics. Geophysical Monographs 40, 221-227.

Ernst, W.G., 1975. Systematics of large-scale tectonics and age progressions in Alpine Circum-Pacific blueschist belts. Tectonophysics 26, 229-246.

Franzese, J., 1994. El metamorfismo Neopaleozoico del sector Andino entre los 38°-40° LS. Un Cinturon oblicuo a la cadena actual? 7. Congreso Geológico Chileno, Universidad de Concepción, Actas, Vol. 2, pp. 1341-1343.

Franzese, J.R., Spalletti, L.A., 2001. Late Triassic-early Jurassic continental extension in southwestern Gondwana: tectonic segmentation and pre-break-up rifting. Journal of South American Earth Sciences 14, 257-270.

Freeman, S.R., Inger, S., Butler, R.W.H., Cliff, R.A., 1997. Dating deformation using Rb-Sr in white mica: greenschist facies deformation ages from the Entrelor shear zone, Italian Alps. Tectonics 16, 57-76.

Glodny, J., Grauert, B., Fiala, J., Vejnar, Z., Krohe, A., 1998. Metapegmatites in the western Bohemian massif: ages of crystallization and metamorphic overprint, as constrained by U-Pb zircon, monazite, garnet, columbite and Rb-Sr muscovite data. Geologische Rundschau 87, 124-134.

Glodny, J., Lohrmann, J., Echtler, H., Gräfe, K., Seifert, W., Collao, S., Figueroa, O., 2005. Internal dynamics of a paleoaccretionary wedge: insights from combined isotope tectonochronology and sandbox modelling of the South-Central Chilean forearc. Earth and Planetary Science Letters 231, 23-39.

Glodny, J., Echtler, H., Figueroa, O., Franz, G., Gräfe, K., Kemnitz, H., Kramer, W., Krawczyk, C., Lohrmann, J., Lucassen, F., Melnick, D., Rosenau, M., Seifert, W. 2006. Long-term geological evolution and mass flow balance of the South-Central Andes. In: Oncken, O., Chong, G., Franz, G., Giese, P., Götze, H.-J., Ramos, V., Strecker, M., Wigger, P. (eds): The Andes – active subduction orogeny. Frontiers in Earth Sciences, Vol. 1, Springer Verlag, p. 401-428.

Glodny, J., Gräfe, K., Echtler, H., Rosenau, M. 2008. Mesozoic to Quaternary continental margin dynamics in South Central Chile (36°-42°S): the apatite and zircon fission track perspective. International Journal of Earth Sciences, doi:10.1007/s00531-007-0203-1 (in press)

Godoy, E., Kato, T., 1990. Late Paleozoic serpentinites and mafic schists from the Coast Range accretionary complex, central Chile: their relation to aeromagnetic anomalies. Geologische Rundschau 79, 121-130.

González-Bonorino, F., Aguirre, L., 1970. Metamorphic facies series of the crystalline basement of Chile. Geologische Rundschau 59, 979-994.

González-Bonorino, F., 1971. Metamorphism of the crystalline basement of central Chile. Journal of Petrology 12, 149-175.

Gutscher, M.-A., Kukowski, N., Malavieille, J., Lallemand, S., 1998. Episodic imbricate thrusting and underthrusting: Analog experiments and mechanical analysis applied to the Alaskan Accretionary Wedge. Journal of Geophysic Research 103, 10161-10176.

Hervé, F., 1977. Petrology of the crystalline basement of the Nahuelbuta mountains, southcentral Chile, in: Ishikawa, T., Aguirre L. (Eds). Comparative studies on the geology of the Circum-Pacific Orogenic Belt in Japan and Chile. Japan Society for the Promotion of Science, Tokyo, pp. 1-51.

Hervé, F., 1988. Late Paleozoic subduction and accretion in Southern Chile. Episodes 11, 183-188.

Hervé, F., Moreno, H., Parada, M.A., 1974. Granitoids of the Andean Range of Valdivia province, Chile. Pacific Geology 8, 39-46.

Hervé, F., Thiele, R., Parada, M.A., 1976. Observaciones geológicas en el Triásico de Chile central entre las latitudes 35°30' y 40°00' sur. Congreso Geologico Chileno I, A297-313, Santiago.

Hervé, F., Godoy, E., Parada, M.A., Ramos, V., Rapela, C., Mpodozis, C., Davidson J., 1987. A general view of the Chilean-Argentinian Andes, with emphasis on their early history, in: Monger, J.W.H., & Francheteau, J., (Eds.), Circum-Pacific Orogenic Belts and Evolution of the Pacific Ocean Basin. AGU, Geodynamics Series 18, pp. 97-114.

Hervé, F., Munizaga, F., Parada, M.A., Brook, M., Pankhurst, R.J., Snelling, N.J., Drake, R., 1988. Granitoids of the Coast Range of central Chile: Geochronology and geologic setting. Journal of South American Earth Sciences 1, 185-194.

Hervé, F., Fanning, C.M., Pankhurst, R.J., 2003. Detrital zircon age patterns and provenance of the metamorphic complexes of southern Chile. Journal of South American Earth Sciences 16, 107-123.

Höfer, C., Kraus, S., Miller, H., Alfaro, G., Barra, F., 2001. Chromite-bearing serpentinite bodies within an arc-backarc metamorphic complex near La Cabana, south Chilean Coastal Cordillera. Journal of South American Earth Sciences 14, 113-126.

Kato, T.T., 1976. The relationship between low-grade metamorphism and tectonics in the Coast Range of Central Chile. Dissertation, University of California, Los Angeles p. 238.

Kato, T.T., 1985. Pre-Andean orogenesis in the Coast Ranges of Central Chile. Geological Society of America, Bulletin 96, 918-924.

Kato, T.T., Godoy, E., 1995. Petrogenesis and tectonic significance of Late Paleozoic coarse-crystalline blueschist and amphibolite boulders in the coastal range of Chile. International Geology Review 37, 992–1006.

Krawczyk, C.M., and the SPOC Team, 2003. Amphibious seismic survey images plate interface at 1960 Chile earthquake. EOS 84, 304-305.

Kullerud, L., 1991. On the calculation of isochrons. Chemical Geology 87, 115-124.

Laursen, J., Scholl, D.W., von Huene, R., 2002. Neotectonic deformation of the central Chile margin: Deepwater forearc basin formation in response to hot spot ridge and seamount subduction. Tectonics 21(5), 1038, doi:10.1029/2001TC901023.

Levi, B., Aguilar, A., Fuenzalida, R., 1966. Reconocimiento geológico en las provincias de Llanquihue y Chiloé. Instituto de Investigaciones Geológicas (ILG), Chile, Boletin, 19, p. 45.

Lohrmann, J., 2002. Identification of parameters controlling the accretive and tectonically erosive mass-transfer mode at the South-Central and North Chilean forearc using scaled 2D sandbox experiments, Dissertation, FU Berlin, 2002, Scientific Technical Report STR02/10, http://www.gfz-potsdam.de/bib/zbstr.htm.

Lucassen, F. , Trumbull, R. , Franz, G., Creixell, C., Vásquez, P., Romer, R.L., Figueroa, O., 2004. Distinguishing crustal recycling and juvenile additions at active continental margins: the Paleozoic to recent compositional evolution of the Chilean Pacific margin (36°-41°S). Journal of South American Earth Sciences 17, 103-119.

Ludwig, K.R., 1999. Isoplot/Ex Ver 2.06: A geochronological toolkit for Microsoft Excel. Berkeley Geochronology Center Special Publications 1a.

Martin, M.W., Kato, T.T., Campos, A., 1997. Stratigraphic, structural, metamorphic and timing constraints for the assembly of Late Paleozoic to Triassic rocks in the Lake district, Chile (~40°S). VIII. Congreso Geológico Chileno, Universidad Catolica del Norte, Actas Vol. 1, 154-158.

Martin, M.W., Kato, T.T., Rodriguez, C., Godoy, E., Duhart, P., McDonough, M., Campos, A., 1999. Evolution of the late Paleozoic accretionary complex and overlying forearc-magmatic arc, south central Chile (38°-41°S): Constraints for the tectonic setting along the southwestern margin of Gondwana. Tectonics 18, 582-605.

Miyashiro, A., 1961. Evolution of metamorphic belts. Journal of Petrology 2, 277-311.

Moore, J.C., Silver, E.A., 1987. Continental margin tectonics; submarine accretionary prisms. Reviews of Geophysics 25, 1305-1312.

Mpodozis, C., Ramos, V.A., 1989. The Andes of Chile and Argentina, in: Ericksen, G.E., Cañas Pinochet, M.T., Reinemund, J.A. (Eds.) Geology of the Andes and its relation to Hydrocarbon and Mineral Resources. Circumpacific Council for Energy and Mineral Resources, Earth Sciences Series 11, pp. 59-90.

Pankhurst, R.J., Hervé, F., Rojas, L., Cembrano, J., 1992. Magmatism and tectonics in continental Chiloé, Chile (42°-42°30'S). Tectonophysics 205, 283-294.

Parada, M.A., 1975. Estudio geológico de los alrededores de los lagos Calafquén, Panguipulli y Riñihue, Provincia de Valdivia. Memoria de título, Departamento de Geologia, Universidad de Chile, Santiago, p. 106 .

Rapela, C.W., Pankhurst, R.J., 1992. The granites of northern Patagonia and the Gastre Fault System in relation to the break-up of Gondwana, in: Storey, B.C., Alabaster, T., and Pankhurst, R.J., (Eds.), Magmatism and the causes of continental break-up. Geological Society Special Publication 68, pp. 209-220.

Rehak K., Strecker M., Echtler, H., 2008. Morphotectonic segmentation of an active forearc, 37°–41°S, Chile. Geomorphology 94, 98-116.

Richter, P.P., Ring, U., Willner, A.P., Leiss, B., 2007. Structural contacts in subduction complexes and their tectonic significance: the Late Paleozoic coastal accretionary wedge of Central Chile. Journal of the Geological Society, London 164, 203-214.

Rosenau, M.R., 2004. Tectonics of the Southern Andean Intra-arc Zone (38° - 42°S). Dissertation, Freie Universität Berlin, http://www.diss.fu-berlin.de/2004/280/index.html, 154 p.

SERNAGEOMIN, 2003. Mapa Geológico de Chile: versión digital. Servicio Nacional de Geología y Minería, Publicación Geológica Digital, No. 4 (CD-ROM, versión1.0, 2003), Santiago de Chile.

Shepherd, T.J., 1981. Temperature programmable heating-freezing stage for microthermometric analysis of fluid inclusions. Economic Geology 76, 1244-1247.

Stöckhert, B., Brix, M.R., Kleinschrodt, R., Hurford, A.J., Wirth, R., 1999. Thermochronometry and microstructures of quartz - a comparison with experimental flow laws and predictions on the temperature of the brittle-plastic transition. Journal of Structural Geology 21, 351-369.

Varela, R., Teixeira, W., Cingolani, C., Dalla Salda, L., 1994. Edad Rubidio-Estroncio de granitoides de Alumine-Rahue, Cordillera Norpatagonica, Neuquen, Argentina. 7. Congreso Geologico Chileno, Universidad de Concepción, Actas Vol. 2, pp. 1254-1258.

Villa, I.M., 1998. Isotopic closure. Terra Nova 10, 42-47.

Von Blanckenburg, F., Villa, I.M., Baur, H., Morteani, G., Steiger, R.H., 1989. Time calibration of a P-T path from the Western Tauern Window, Eastern Alps: the problem of closure temperatures, Contributions to Mineralogy and Petrology 101, 1-11.

Von Gosen, W., Loske, W., 2004. Tectonic history of the Calcatapul Formation, Chubut province, Argentina, and the “Gastre fault system”. Journal of South American Earth Sciences 18 , 73-88.

Von Huene, R., Scholl, D.W., 1991. Observations at convergent margins concerning sediment subduction, subduction erosion, and the growth of continental crust. Reviews of Geophysics 29(3), 279-316.

Von Huene, R., Ranero, C.R., 2003. Subduction erosion and basal friction along the sediment-starved convergent margin off Antofagasta, Chile. Journal of Geophysical Research 108(B2), 2079, doi:10.1029/2001JB001569.

Von Huene, R., Corvalán, J., Flueh, E.R., Hinz, K., Korstgard, J., Ranero, C.R., Weinrebe, W., and the CONDOR Scientists, 1997. Tectonic control of the subducting Juan Fernández Ridge on the Andean margin near Valparaiso, Chile. Tectonics 16(3), 474-488.

Willner A.P., 2005. Pressure Temperature evolution of a Late Paleozoic paired metamorphic belt in North-Central Chile (34°-35°30’S). Journal of Petrology 46(9), 1805-1833.

Willner, A.P., Hervé, F., Massonne, H.J., 2000. Mineral chemistry and pressure-temperature evolution of two contrasting high-pressure-low-temperature belts in the Chonos archipelago, Southern Chile. Journal of Petrology 41, 309-330.

Willner, A.P., Pawlig, S., Massonne, H.J., Hervé, F., 2001. Metamorphic evolution of spessartine quartzites (coticules) in the high-pressure, low temperature complex at Bahia Mansa, Coastal Cordillera of South-Central Chile. Canadian Mineralogist 39, 1547-1569.

Willner, A.P., Glodny, J., Gerya, T.V., Godoy, E., Massonne, H.J., 2004. A counterclockwise PTt-path of high pressure-low temperature rocks from the Coastal Cordillera accretionary complex of South Central Chile: constraints for the earliest stage of subduction mass flow. Lithos 75, 283-310.

Willner, A.P., Thomson, S.N., Kröner, A., Wartho, J.-A., Wijbrans J.R., Hervé, F., 2005. Time markers for the evolution and exhumation history of a Late Paleozoic paired metamorphic belt in North-Central Chile (34°-35°30'S). Journal of Petrology 46(9), 1835-1858.

Yáñez, G.A., Ranero, C.R., von Huene, R., Díaz J., 2001. Magnetic anomaly interpretation across the southern central Andes (32°-34°S): The role of the Juan Fernández Ridge in the Late Tertiary evolution of the margin. Journal of Geophysical Research 106(B4), 6325-6345.

Figure captions

Fig. 1. Schematic geological map of pre-Jurassic units in South Central Chile (34°S - 42°S).

Fig. 2 Geological map of the Cordillera Nahuelbuta area, South Central Chile, with isotopic age data. Map modified after SERNAGEOMIN (2003).

Fig. 3. a) Andalusite porphyroblasts, postkinematic with respect to S_1. The big crystal is ~0.5 mm across. Roadcut between Cap. Pastene and Lumaco. b) Staurolite schist (equivalent to sample VAL65s), with mm-sized staurolite crystals, influenced by Lanalhue fault activity. Staurolite growth is pre-tectonic with respect to S_2. Reaction texture, formed by retrograde staurolite breakdown to chlorite+sericite along grain boundaries and cracks. Matrix of quartz, biotite, chlorite, white mica, and occasionally actinolitic amphibole. c) Filled tension gash (sample VAL65), kinematically related to S_2 development and Lanalhue fault activity. Mineralization is quartz-dominated, with sparse white mica, feldspar and chlorite. Long axis of hammerhead (for scale): 13 cm. d) Massive quartz mineralization within the Lanalhue Fault Zone, with nearly monomineralic quartz enclosing wallrock fragments. Outcrop near Capitán Pastene. e) Field aspect of Eastern Series samples VAL60a (mobilisate) and VAL60c (schist, deformed and bent around the mobilisate). Mobilisate formation predates lasts increments of regional deformation. Both samples come from coastal cliffs south of Playa Chivilingo. Long axis of hammerhead (for scale): 13 cm. f) Western Series. Extensional, semiductile shear zone in Western Series schists. Sample VAL61, Cabo Tirúa, SW of Tirúa. Hammer handle (for scale): 30 cm.

Fig. 4. Map view and profile, Lanalhue Fault Zone near Capitán Pastene (cf. Fig. 2), with structural inventory. Map shows foliation deflection in the fault zone area, indicating a sinistral sense of shear. Equal-area stereonet projections show orientation of foliations, microfold axes and stretching lineations within the Lanalhue Fault Zone. See text for discussion.

Fig. 5. Rb/Sr mineral isochron age data, Lanalhue Fault Zone. Sample VAL63 is part of an extensive quartz mineralization within the trace of the fault. VAL64 and VAL65 are from late, discordant tension gashes. VAL65S is Eastern Series with deformation related to Lanalhue fault activity. VAL62 is a Western Series schist, distant to the fault trace. Abbreviations: wm: white mica; nm: nonmagnetic separate (Frantz 0.55A/13°)

Fig. 6. Schematic model of Lanalhue fault evolution, with vertically exaggerated cross sections of the continental margin at ~40°S. a) at ~305 Ma, shortly after onset of subduction. Formation of the Eastern Series by thrusting and frontal accretion of thick, turbiditic, former passive margin sediments. Incipient growth of a basal accretionary complex (Western Series), partly by return flow from the subduction channel (cf. Willner et al., 2004). b) ~300 Ma. Continuing deformation of Eastern Series, basal growth of Western Series, both contemporaneous with arc magmatism. Normal fault contact between Eastern and Western Series in the Eastern flank of the Western Series. c) ~290 Ma. Waning stage of arc magmatism. Deformation of Eastern Series close to the contact to the Western Series has ceased. Continuous growth and denudation of the Western Series. Western Series most probably exposed at the surface, with undisturbed, NNE-SSW trending normal fault contact in its eastern flank towards the Eastern Series. d) ~275 Ma. Ongoing Western Series basal accretion south of 38°S contrasts with subduction erosion and forearc mass wasting further north. Differential margin behaviour triggers margin segmentation, with reworking of the Western Series-Eastern Series contact as a sinistral semiductile to brittle transform fault.

Tables

Table 1. Rb/Sr analytical data.

Sample No. Analysis No.	Material	Rb [ppm]	Sr [ppm]	$^{87}Rb/^{86}Sr$	$^{87}Sr/^{86}Sr$	$^{87}Sr/^{86}Sr$ $2\sigma_m$ [%]
Quartz mineralization in the trace of the Lanalhue Fault Zone						
VAL63 (274.4 ± 2.5 Ma, MSWD = 1.8, Sr_i = 0.719695 ± 0.000056)						
PS758	wm 200 - 500 µm	589	175	9.81	0.757611	0.0012
PS768	wm 125 - 200 µm	593	177	9.73	0.757637	0.0012
PS769	quartz + chlorite + wm	25.3	10.9	6.74	0.746271	0.0014
PS805	quartz	0.13	0.67	0.579	0.721956	0.0014
Tension gashes (related to S_2), Lanalhue Fault Zone						
VAL65 (271.6 ± 3.5 Ma, MSWD = 0.36, Sr_i = 0.717075 ± 0.000054)						
PS755	wm 250 - 500 µm	193.	178	3.14	0.729252	0.0012
PS793	feldspar	47.5	312	0.441	0.718779	0.0012
PS796	wm 125 - 250 µm	198	173	3.33	0.729896	0.0014
PS790(*)	chlorite	1.95	2.08	2.72	0.724413	0.0042
VAL64 (280.3 ± 6.4 Ma, MSWD = 22, Sr_i = 0.7185 ± 0.0010)						
PS754	wm 200 - 500 µm	505	81.4	18.1	0.791325	0.0012
PS772	quartz 1	0.13	3.66	0.100	0.718943	0.0014
PS778	quartz 2	0.28	3.58	0.225	0.719238	0.0014
PS784	wm > 500 µm	474	81.7	16.9	0.786062	0.0016
PS789	wm 125 - 200 µm	505	77.7	19.0	0.793063	0.0012
Eastern Series rocks, influenced by Lanalhue Fault activity						
VAL65S (274 ± 12 Ma, MSWD = 35, Sr_i = 0.7173 ± 0.0025)						
PS820	whole rock	168	130	3.75	0.732510	0.0016
PS821	biotite	506	32.9	45.3	0.894301	0.0012
PS824	sep. nm 0.55A/13°	147	141	3.02	0.729447	0.0016
PS827	chlorite	8.54	4.62	5.37	0.737217	0.0020
Western Series						
VAL62 (272.7 ± 2.8 Ma, MSWD = 1.8, Sr_i = 0.711932 ± 0.000025)						
PS774	feldspar (albite)	1.96	127	0.0448	0.712082	0.0014
PS777	epidote + titanite	7.53	311	0.0700	0.712228	0.0016
PS780	wm 180 - 355 µm	345	55.2	18.2	0.782497	0.0012
PS788	wm > 500 µm	364	72.8	14.6	0.768432	0.0012
LAH3 (294.3 ± 9.4 Ma, MSWD = 2.2, Sr_i = 0.71556 ± 0.00091)						
PS1120	wm 125-80 µm	428	156	7.96	0.748491	0.0014
PS1121	wm 160-125 µm	451	163	8.04	0.749701	0.0012
PS1123	feldspar	4.46	92.9	0.139	0.716144	0.0014
PS1124	wm 250-180 µm	460	162	8.26	0.750009	0.0014
PS1126	wm 355-250 µm	460	159	8.39	0.750783	0.0016
Western Series, semiductile extensional shear band						
VAL61 (255.8 ± 2.7 Ma, MSWD = 0.53, Sr_i = 0.718612 ± 0.000035)						
PS787	feldspar, etched in HF	0.87	101.7	0.0249	0.718703	0.0014
PS791	white mica 250-180 µm	493	99.27	14.5	0.770997	0.0016
PS801	white mica >250 µm	498	90.92	16.0	0.776901	0.0014
Eastern Series, Playa Chivilingo						
VAL60a (295 ± 14 Ma, MSWD = 3.3, Sr_i = 0.71302 ± 0.00022)						
PS767	clinozoisite	0.84	1268	0.00193	0.713051	0.0012
PS781	wm 250 - 355 µm	213	359	1.74	0.719310	0.0012
PS785	wm (paragonite), 125 - 250	169	542	0.900	0.716713	0.0010
PS797	wm > 500 µm	216	359	1.74	0.720344	0.0016
VAL60c (294.8 ± 3.4 Ma, MSWD = 0.1, Sr_i = 0.713548 ± 0.000055)						
PS762	wm 180 - 500 µm LBRF	271	88.5	8.90	0.750864	0.0014
PS771	feldspar + quartz	75.5	446	0.490	0.715603	0.0012
PS792	wm HBRF	182	123	4.45	0.732202	0.0012
Magmatic and migmatic rocks, Cordillera Nahuelbuta						
FLO1 (306.8 ± 4.5 Ma, Sr_i = 0.7083 ± 0.0022)						
PS 339	feldspar	276	34.1	23.7	0.811835	0.0016
PS 372	muscovite 3 x 0.5 cm	1220	2.45	3750	17.05845	0.0020
NPN2 (297.3 ± 2.5 Ma, MSWD = 1.7, Sr_i = 0.714198 ± 0.000036)						
PS657	biotite > 500 µm	498	4.83	341	2.145680	0.0030
PS659	wm m = 0.81 A	208	48.4	12.5	0.766749	0.0016
PS661	wm nm = 0.81 A	197	46.7	12.3	0.766716	0.0018
PS700	quartz + feldspar	5.83	168	0.101	0.714623	0.0016
ANG1 (286.3 ± 4.2 Ma, Sr_i = 0.707117 ± 0.000035)						

PS656	biotite	695	4.94	486	2.685696	0.0040
PS686	feldspar	5.94	289	0.0595	0.707359	0.0014

Errors are reported at the 2σ level. (*): not used for age calculation. An uncertainty of ± 1.5 % is assigned to Rb/Sr ratios. wm: white mica; HBRF: sinks in bromoform (= density >2.82) LBRF: floats in bromoform; sep., separate; m/nm: magnetic/nonmagnetic on Frantz magnetic separator, 13° tilt, at electric current as indicated.

Table 2. Summary of microthermometric results. Quartz mobilisates, Lanalhue Fault Zone

Sample	host mineral	inclusion types	n	T_h [°C] mean ± s.d.	T_h [°C] total range	weight % $NaCl_{eq.}$ (range)
VAL 63	quartz	p,ps,s; L+V	42	154.4 ± 43.0	387-110	0.9-11.8
VAL 64	quartz	p,ps,s; L+V	38	171.5 ± 47.8	309.9-92.6	5.3-18.3

Analyses realized in the microthermometry laboratory at the Departamento de Ciencias de la Tierra, Universidad de Concepción, using a Linkam TH-600 heating and freezing stage. T_h, homogenization temperature; n, number of analyzed inclusions; p, primary; ps, pseudosecondary; s, secondary; L+V: liquid + vapor.

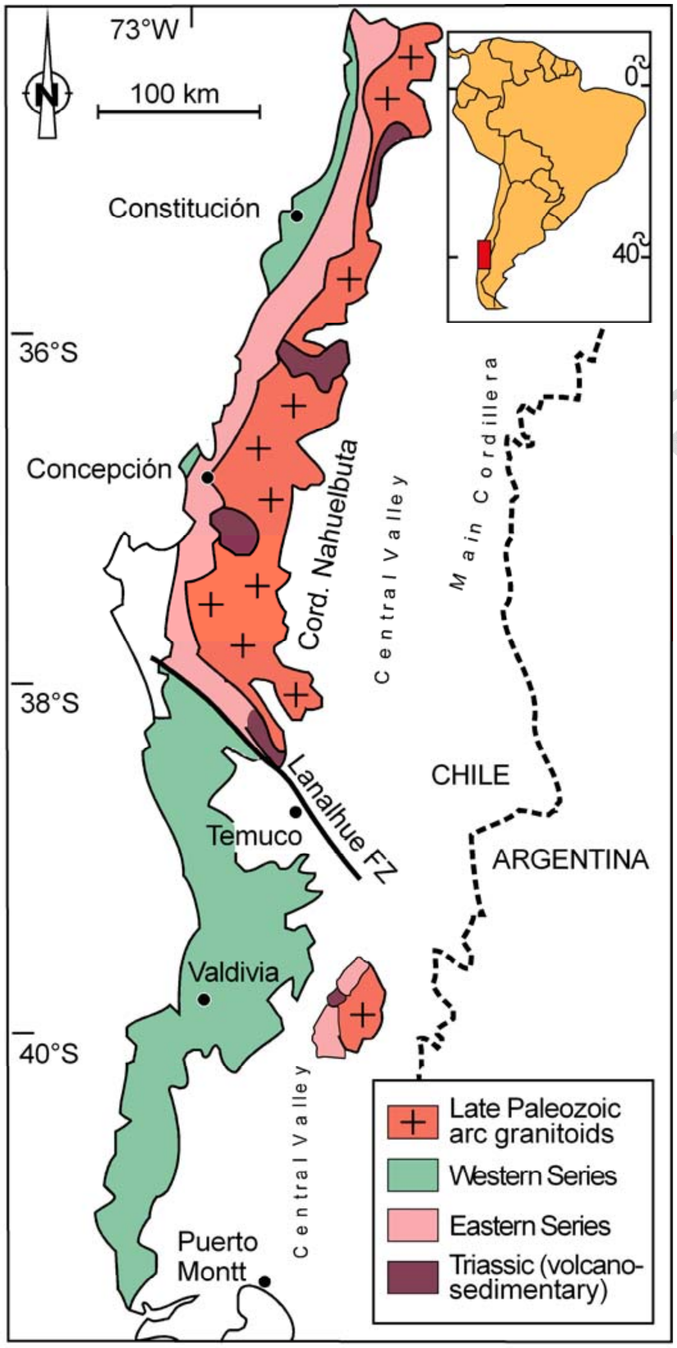
73°W
N
100 km
Constitución
36°S
Concepción
Cord. Nahuelbuta
Central Valley
Main Cordillera
38°S
Lanalhue FZ
CHILE
Temuco
ARGENTINA
Valdivia
40°S
Central Valley
Puerto Montt
0
40
Late Paleozoic arc granitoids
Western Series
Eastern Series
Triassic (volcano-sedimentary)

1119 .

1120
1121

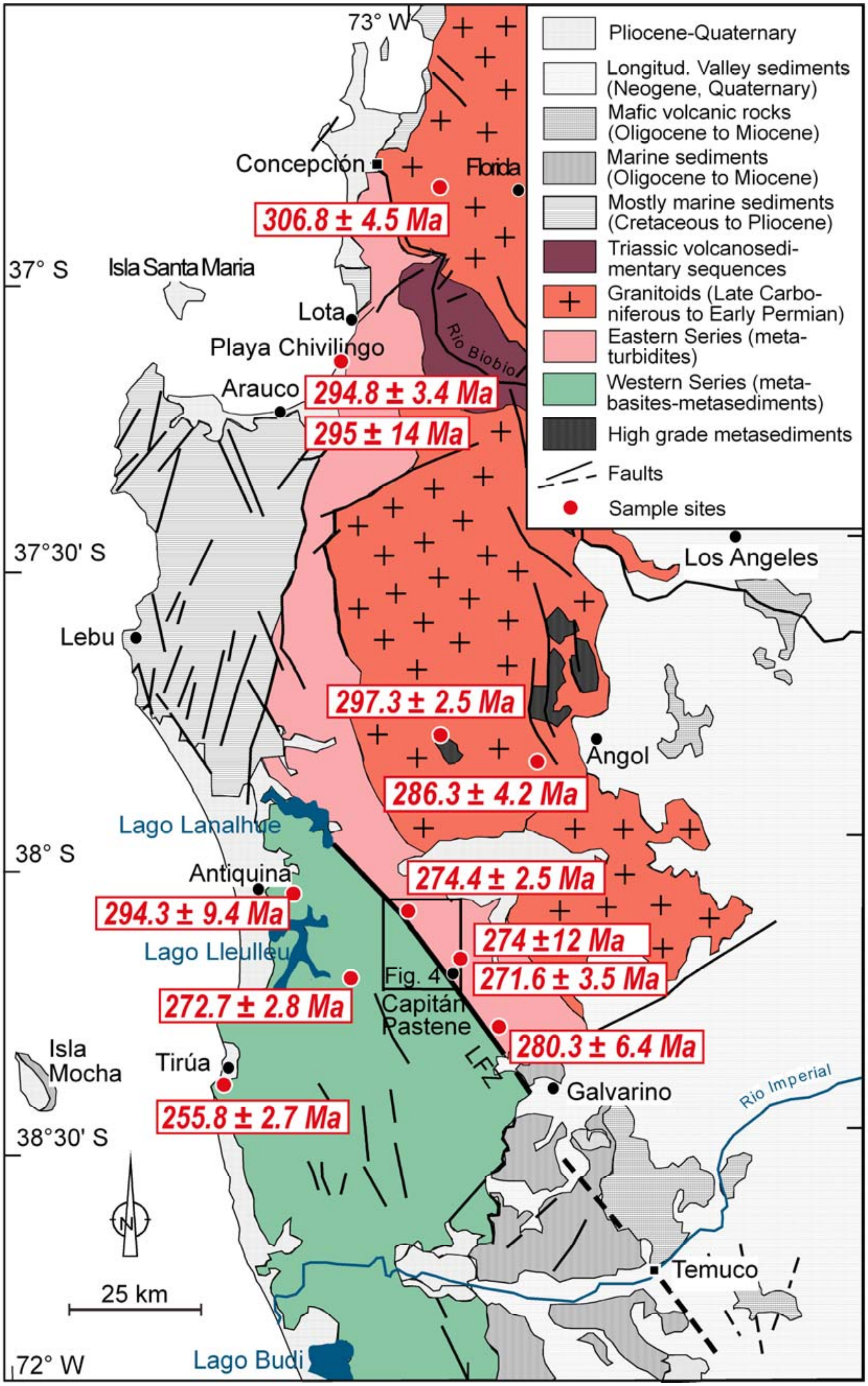

1122

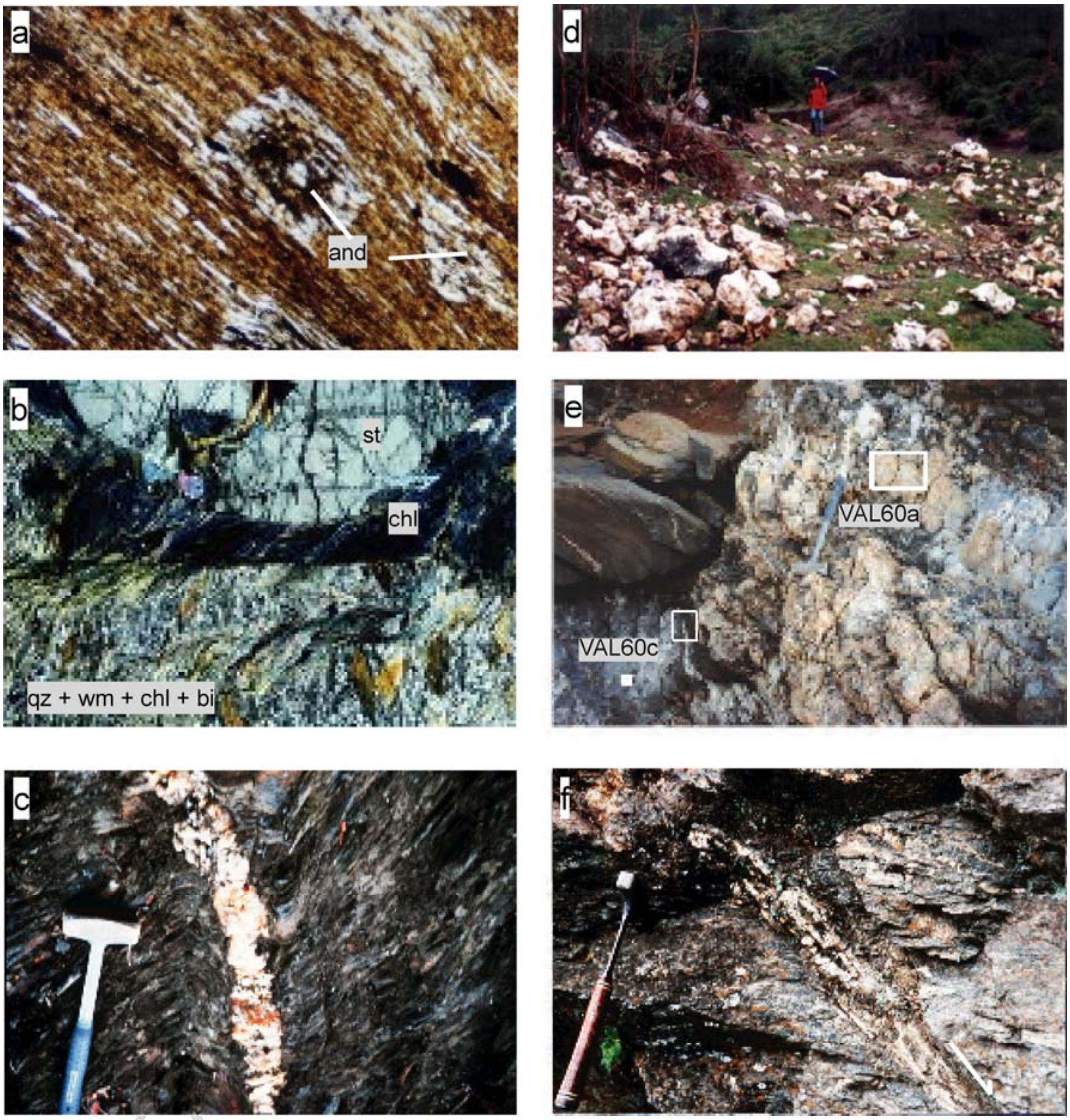
a
and
d
b
st
chl
qz + wm + chl + bi
e
VAL60a
VAL60c
c
f

1126
1127

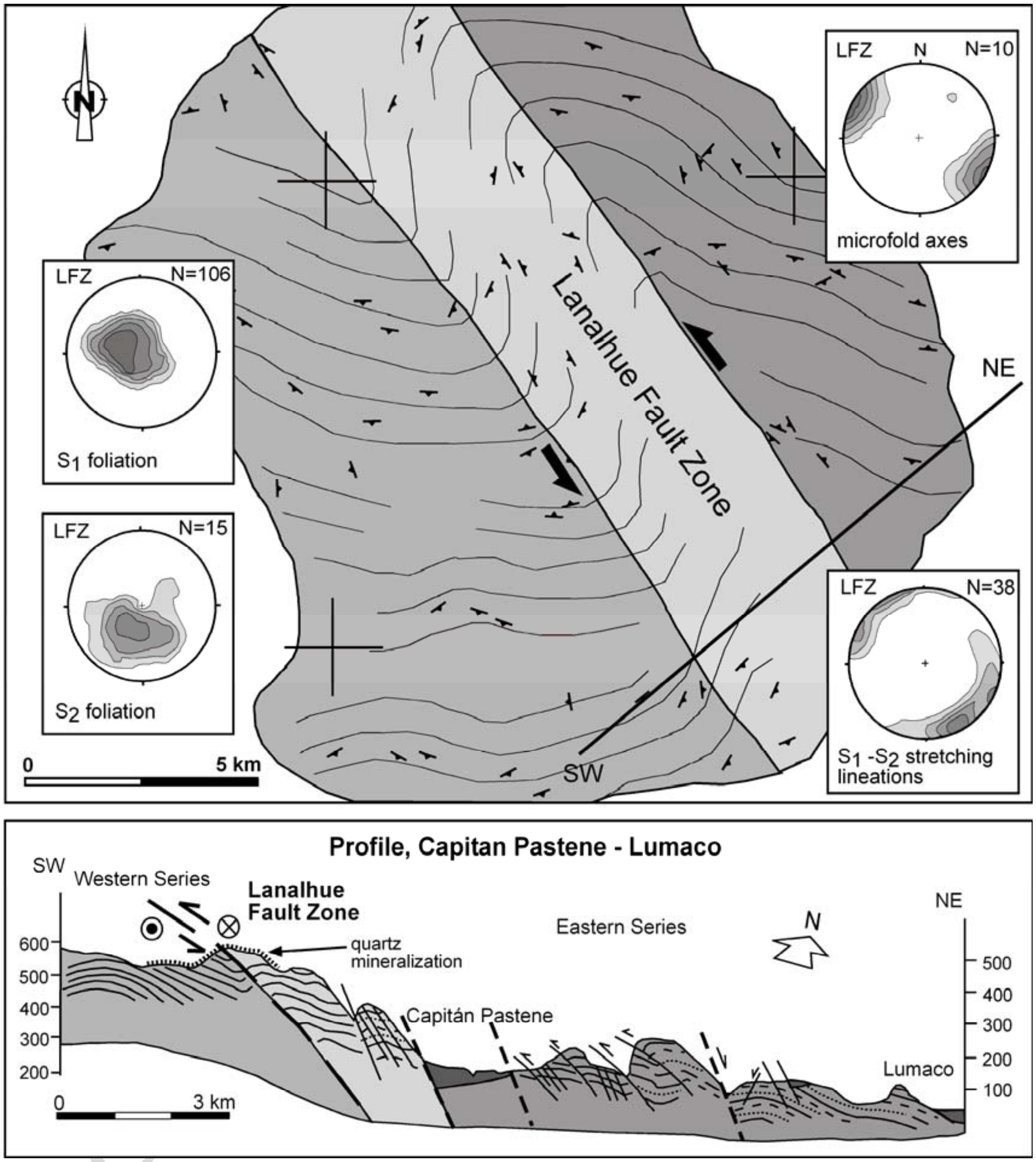

1128

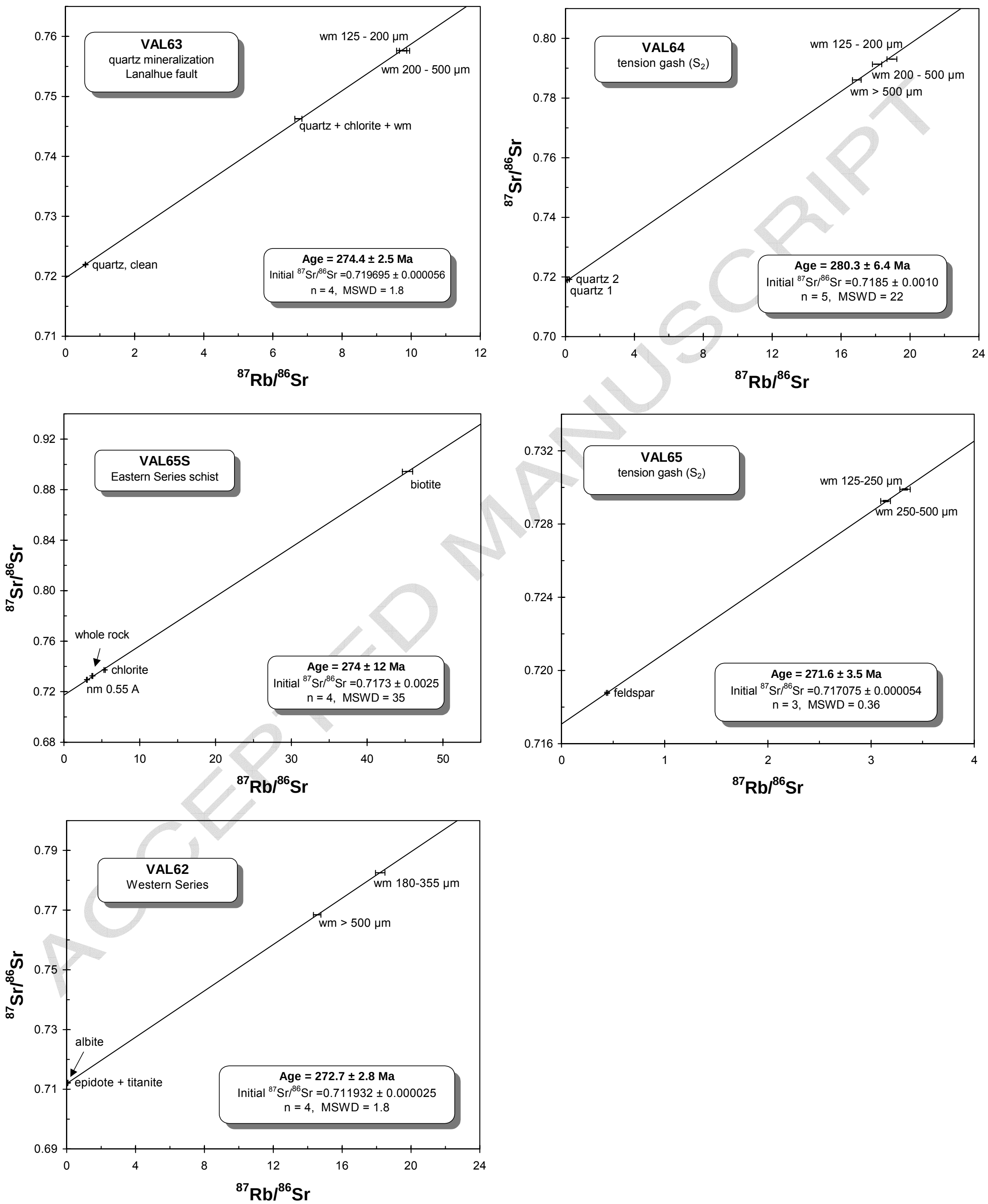
VAL63
quartz mineralization
Lanalhue fault
wm 125 - 200 µm
wm 200 - 500 µm
quartz + chlorite + wm
quartz, clean
Age = 274.4 ± 2.5 Ma
Initial 87Sr/86Sr =0.719695 ± 0.000056
n = 4, MSWD = 1.8
87Rb/86Sr
VAL64
tension gash (S2)
wm 125 - 200 µm
wm 200 - 500 µm
wm > 500 µm
quartz 2
quartz 1
Age = 280.3 ± 6.4 Ma
Initial 87Sr/86Sr =0.7185 ± 0.0010
n = 5, MSWD = 22
87Sr/86Sr
87Rb/86Sr
VAL65S
Eastern Series schist
biotite
whole rock
chlorite
nm 0.55 A
Age = 274 ± 12 Ma
Initial 87Sr/86Sr =0.7173 ± 0.0025
n = 4, MSWD = 35
87Sr/86Sr
87Rb/86Sr
VAL65
tension gash (S2)
wm 125-250 µm
wm 250-500 µm
feldspar
Age = 271.6 ± 3.5 Ma
Initial 87Sr/86Sr =0.717075 ± 0.000054
n = 3, MSWD = 0.36
87Rb/86Sr
VAL62
Western Series
wm 180-355 µm
wm > 500 µm
albite
epidote + titanite
Age = 272.7 ± 2.8 Ma
Initial 87Sr/86Sr =0.711932 ± 0.000025
n = 4, MSWD = 1.8
87Sr/86Sr
87Rb/86Sr

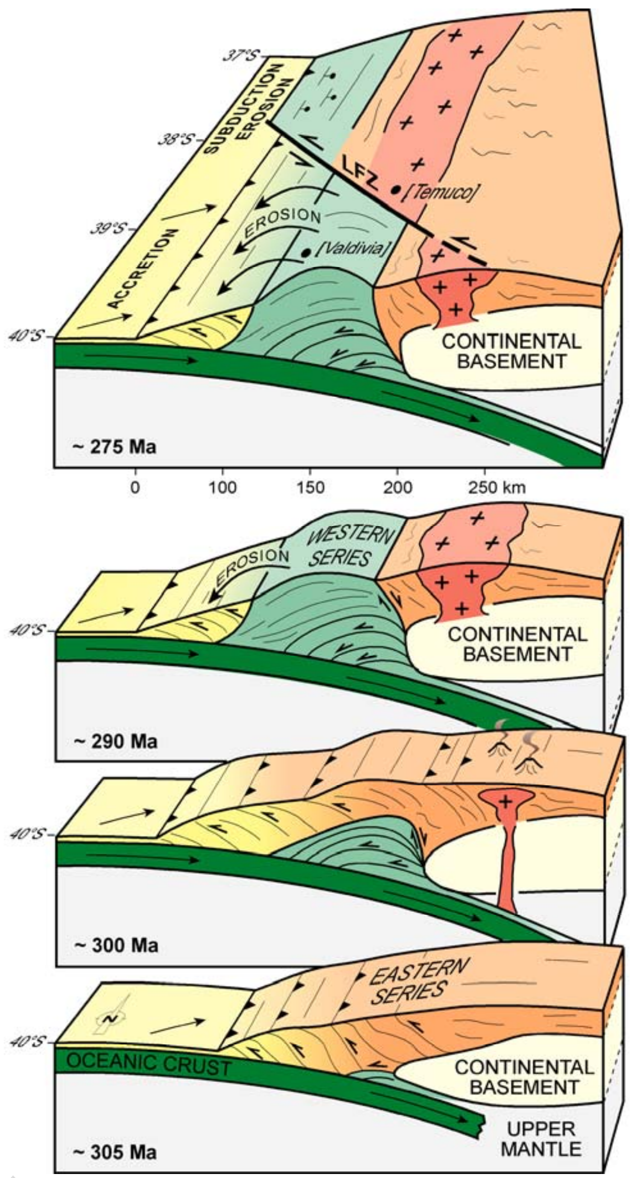
37°S
38°S
39°S
40°S
SUBDUCTION EROSION
ACCRETION
EROSION
LFZ
[Temuco]
[Valdivia]
CONTINENTAL BASEMENT
~ 275 Ma
0
100
150
200
250 km
WESTERN SERIES
EROSION
40°S
CONTINENTAL BASEMENT
~ 290 Ma
40°S
~ 300 Ma
EASTERN SERIES
40°S
N
OCEANIC CRUST
CONTINENTAL BASEMENT
UPPER MANTLE
~ 305 Ma